Performance of an intra-train dual-phase feedback system at KEK ATF2

D. R. Bett,* P. N. Burrows, C. Perry, and R. Ramjiawan
John Adams Institute for Accelerator Science at University of Oxford,
Denys Wilkinson Building, Keble Road,
Oxford OX1 3RH, United Kingdom

(Dated: May 2, 2019)

A beam orbit correction system has been developed for the extraction line of the Accelerator Test Facility at the High Energy Accelerator Research Organization in Japan. Working with trains of two bunches separated in time by 187.6 ns, the feedback system uses the measured position of the first bunch at two beam position monitors (BPMs) to drive a pair of corrective kicks at two upstream kickers, thus correcting both position and trajectory angle offsets of the second bunch in the vertical axis. The feedback system is shown to be capable of stabilizing the beam offset at the feedback BPMs to within 300 nm and the trajectory angle to within 140 nrad. The quality of the correction has been verified using a witness BPM located 25 m downstream of the kickers as well as a pair of independent BPMs located near the focal point of the machine. Measurements from these witness BPMs are compared with the result of propagating the measurements at the feedback BPMs using a linear model of the lattice and found to be in good agreement.

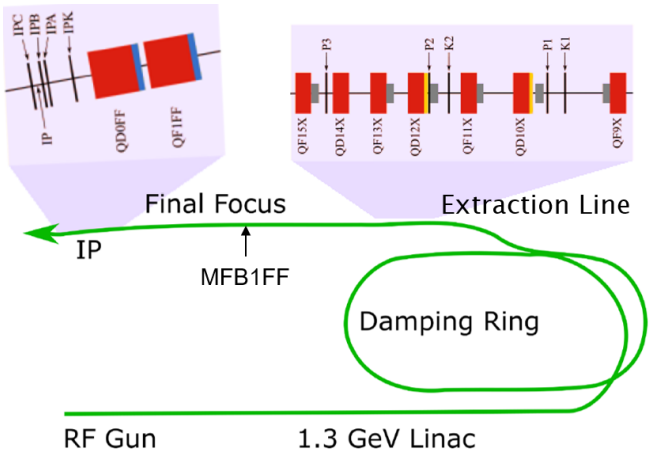

FIG. 1. Layout of the ATF. The label "IP" refers to the nominal interaction point of the machine where the beam size is at a minimum.

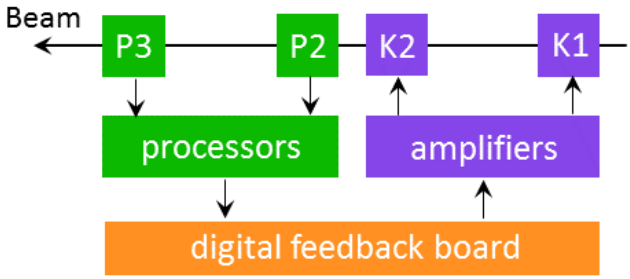

FIG. 2. Schematic of the coupled-loop feedback system using BPMs P2 and P3 and kickers K1 and K2.

I. INTRODUCTION

The Accelerator Test Facility (Figure 1) is a 1.3 GeV electron test accelerator with a repetition rate of 3.12 Hz. It is intended to facilitate the development of the technology and techniques that would be required for a future linear electron-positron collider. The ATF2 Collaboration has two goals: to produce a 37 nm vertical beam spot size at the focal point of the machine and to stabilize the vertical beam position at the same location to the nanometre level.

In pursuit of the beam stabilization goal, the Feedback On Nanosecond Timescales (FONT) group at the University of Oxford has developed a beam position stabilization system. This feedback system is capable of stabilizing both the beam position and trajectory angle in the vertical plane. The corrections are applied locally in the extraction line so that a stable beam is delivered to the entrance of the final focus line.

II. EXPERIMENTAL SETUP

A. Feedback system

The system is depicted schematically in Figure 2. P2 and P3 are beam position monitors (BPMs) of the stripline type. The voltage pulses induced on the top and bottom striplines by the passage of the bunch are processed using custom analogue electronics modules to produce a difference signal (Δ) which depends on the bunch charge and the vertical position of the beam and a sum signal (Σ) which only depends on the bunch charge. The position of the bunch is then proportional to the ratio Δ/Σ. The stripline BPMs and associated processing electronics are the subject of a previously published paper [1]. Here it is noted that the system was upgraded in 2016, resulting in an improved position resolution of

* douglas.bett@physics.ox.ac.uk

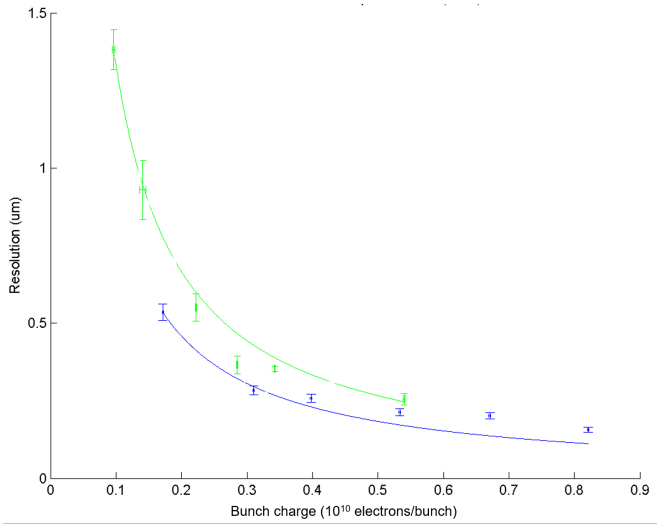

FIG. 3. BPM resolution as a function of beam intensity. The green and blue data points correspond to pre-upgrade and post-upgrade respectively. The lines show the result of scaling the lowest charge data point so that doubling the charge improves the resolution by a factor of two.

~150 nm (Figure 3) for a charge of 1.3 nC (0.8×10^{10} electrons/bunch).

The processed BPM signals are then input to a custom-made digital feedback board. This board features a Field-Programmable Gate Array (FPGA) along with nine analogue-to-digital converters and a pair of digital-to-analogue converters. The feedback algorithm runs on the FPGA and is able to calculate the appropriate kicker drive signals from the digitized BPM signals. The kicker drive signals are then amplified externally using bespoke ultra-fast amplifiers developed by TMD and applied to the stripline kickers K1 and K2. More detail on the digital feedback board and the kicker amplifiers can be found in a second previously published paper [2], which also includes some results of the system operating in a limited mode where a single BPM (P3) was used to drive a single kicker (K2).

Here we consider the fully operational system making use of two BPMs and both kickers. By design each pair of BPM and kicker (P2 and K1, P3 and K2) are situated in the lattice at sufficiently different values of the betatron phase advance that the measurements and corrections are non-degenerate and the offset in both position and trajectory angle can be removed on a train-to-train basis.

B. Feedback algorithm

The feedback algorithm converts the measured position of the first bunch at the feedback BPMs P2 and P3 into a pair of kicks to be applied at the kickers K1 and K2. The corrected position of the second bunch at P2, Y_2'', can be expressed as:

$$Y_2'' = y_2'' + H_{12}v_1 + H_{22}v_2 \tag{1}$$

that is, as the sum of three terms: the first, y_2'', represents the position of bunch 2 at that BPM in the absence of any kicks. The second and third terms correspond to the change in position caused by kicks at K1 and K2 respectively. v_i represents the magnitude of the kick at Ki and H_{ij} is the kicker sensitivity constant that describes how a kick at Ki is converted into a position offset at Pj. A similar expression is obtained for the corrected position of the second bunch at P3 and the two can be expressed together in a single matrix equation:

$$\begin{pmatrix} Y_2'' \\ Y_3'' \end{pmatrix} = \begin{pmatrix} y_2'' \\ y_3'' \end{pmatrix} + \begin{bmatrix} H_{12} & H_{22} \\ H_{13} & H_{23} \end{bmatrix} \begin{pmatrix} v_1 \\ v_2 \end{pmatrix} \tag{2}$$

The goal of the feedback system is to stabilize the position of the second bunch at both BPMs ($Y_2'' = Y_3'' = 0$). It is also assumed that the two bunches are highly correlated such that the uncorrected position of the second bunch is identical to the uncorrected position of the first bunch ($y_j'' = y_j'$). Imposing these conditions leads to the following expression for the kicks:

$$\begin{pmatrix} v_1 \\ v_2 \end{pmatrix} = -\begin{bmatrix} H_{12} & H_{22} \\ H_{13} & H_{23} \end{bmatrix}^{-1} \begin{pmatrix} y_2' \\ y_3' \end{pmatrix} \tag{3}$$

This algorithm is implemented in the firmware of the FONT5 digital processor module in the form:

$$\begin{pmatrix} v_1 \\ v_2 \end{pmatrix} = \begin{bmatrix} G_{21} & G_{31} \\ G_{22} & G_{32} \end{bmatrix} \begin{pmatrix} y_2' \\ y_3' \end{pmatrix} + \begin{pmatrix} \delta v_1 \\ \delta v_2 \end{pmatrix} \tag{4}$$

The feedback parameters G_{ji} represent the extent to which the measured offset at Pj contributes to the kick to be delivered at Ki. They are calculated from the kicker sensitivity constants which are constant for a given set of beam optics and determined empirically. The δv_i term is a constant offset that can be applied to each kick. This allows the mean position of the corrected bunch to be shifted without affecting the reduction in position jitter that can be achieved.

C. Witness BPMs

To verify that the reduction in both position and angle jitter observed at the feedback BPMs survives to the final focus line, a third stripline BPM designated MFB1FF is used as a witness to the correction. This BPM is located about 25 m downstream of the other components (Table I). It is instrumented with the same model of processor module used by P2 and P3 and connected to the same digital feedback board that performs the correction.

To provide a fully independent confirmation, two additional BPMs located close to the focal point of the machine are also used. These BPMs, designated IPA and IPB, are of the cavity type and are instrumented with a completely distinct set of processing electronics, the outputs of which are monitored by a second digital feedback board used purely as a digitizer. A complete description of these BPM electronics can be found in [3].

Here it is noted that the passage of the bunch induces an oscillation of the electric field within the cavity. The first mode of oscillation is proportional to the beam charge while the second mode is proportional to both the beam charge and the transverse position of the beam. The dipole signals from IPA and IPB, along with the monopole signal from a separate reference cavity, are down-mixed to 714 MHz using a frequency-multiplied version of the master RF signal of the ATF damping ring. Each 714 MHz dipole signal is then split in two with one half down-mixed with the 714 MHz reference signal to form a baseband signal denoted I and the other half down-mixed with a 90° phase-shifted version of the 714 MHz reference to form a second baseband signal denoted Q. The position of the bunch is proportional to $I\cos\theta + Q\sin\theta$, where θ is a constant to be determined from calibration.

Variable attenuators on the cavity outputs allow the system to operate for a wide range of beam conditions. Increasing the attenuation increases the dynamic range of the BPMs but degrades the resolution. Typically the BPMs are operated with a resolution of approximately 50 nm and a dynamic range of several microns.

III. FEEDBACK RESULTS

The feedback study was performed using trains of two bunches with a bunch spacing of 187.6 ns. The mean position of the first bunch measured at P2 and P3 was set close to zero by translating those BPMs relative to the beam using the BPM movers. A similar procedure was performed for IPA and IPB which are mounted on a single block that can be both tilted and translated. MFB1FF is not equipped with a mover, resulting in a large offset at that location.

TABLE I. Table indicating the location of selected beamline components in the lattice (relative to the start of the extraction line).

Name	Distance [m]
K1	26.672
K2	29.598
P2	30.123
P3	33.025
MFB1FF	58.534
IPA	89.125
IPB	89.212
IP	89.299

As indicated in Table I, the nominal location of the focal point of the machine is approximately 87 mm downstream of IPB. For this study, the focal point was shifted to be between IPA and IPB by increasing the current of the final focus quadrupole QD0FF. This resulted in a smaller jitter at IPA which made it possible to operate with less attenuation on the cavity outputs, and hence better resolution.

Figure 4 shows the beam distributions recorded at each BPM for a pair of acquisitions, each of which lasted approximately two minutes. The blue and red histograms correspond to feedback off and feedback on respectively. The feedback on data at P2 and P3 shows that the feedback system is kicking the second bunch away from the zero point of those BPMs. Note that this is deliberate and was achieved by using the kick offset terms described in Equation 4 to try and keep the second bunch within the dynamic range of MFB1FF.

The performance of the feedback system can be quantified in a number of ways. Table II shows the measured beam position jitter at each BPM along with the correction factor, defined as the ratio of the jitter of the second bunch in the feedback off run to the jitter of the second bunch in the feedback on run. The jitter achieved at the feedback BPMs themselves is primarily a function of their resolution. The results are consistent with P2 and P3 having an average resolution better than 200 nm. The jitter measured at each witness BPMs is more difficult to interpret. It is clear that the jitter is reduced by a much larger factor at the feedback BPMs (6.5 at P2 and 5.5 at P3) than at the witness BPMs (1.9, 1.8 and 1.6 at MFB1FF, IPA and IPB respectively).

As the system is dual-phase, the effect of the feedback on the angular jitter of the beam is also of interest. The angular jitter is not measured directly but must be inferred using the position measured at two BPMs and knowledge of how the beam is expected to propagate from one BPM to the other. The distribution of angles calculated at P3 using the transfer matrix from P2 to P3 derived from the ATF MAD model is shown in Figure 5. The data suggests the angular jitter at this location is reduced from 1.21 ± 0.04 μrad down to 0.14 ± 0.01 μrad. The angular jitter calculated in the IP region using the position at IPA and IPB is also shown. Here the angular jitter is reduced from a much larger 19.0 ± 0.7 down to 10.9 ± 0.4 μrad. Similarly to the position jitter, the angular jitter is reduced by a much larger factor upstream (8.6) than in the IP region (1.7).

At this point it is helpful to compare the beam distributions measured at the witness BPMs with those predicted by applying the linear transfer matrices to the P2 and P3 data. The two sets of numbers are not in perfect agreement. The estimated jitter at MFB1FF is on average 15% larger than the measurements and the equivalent figure for IPA is close to 30%. Conversely, at IPB the estimated jitter is on average 10% smaller than the measured value. Nevertheless, comparison of the feedback off and

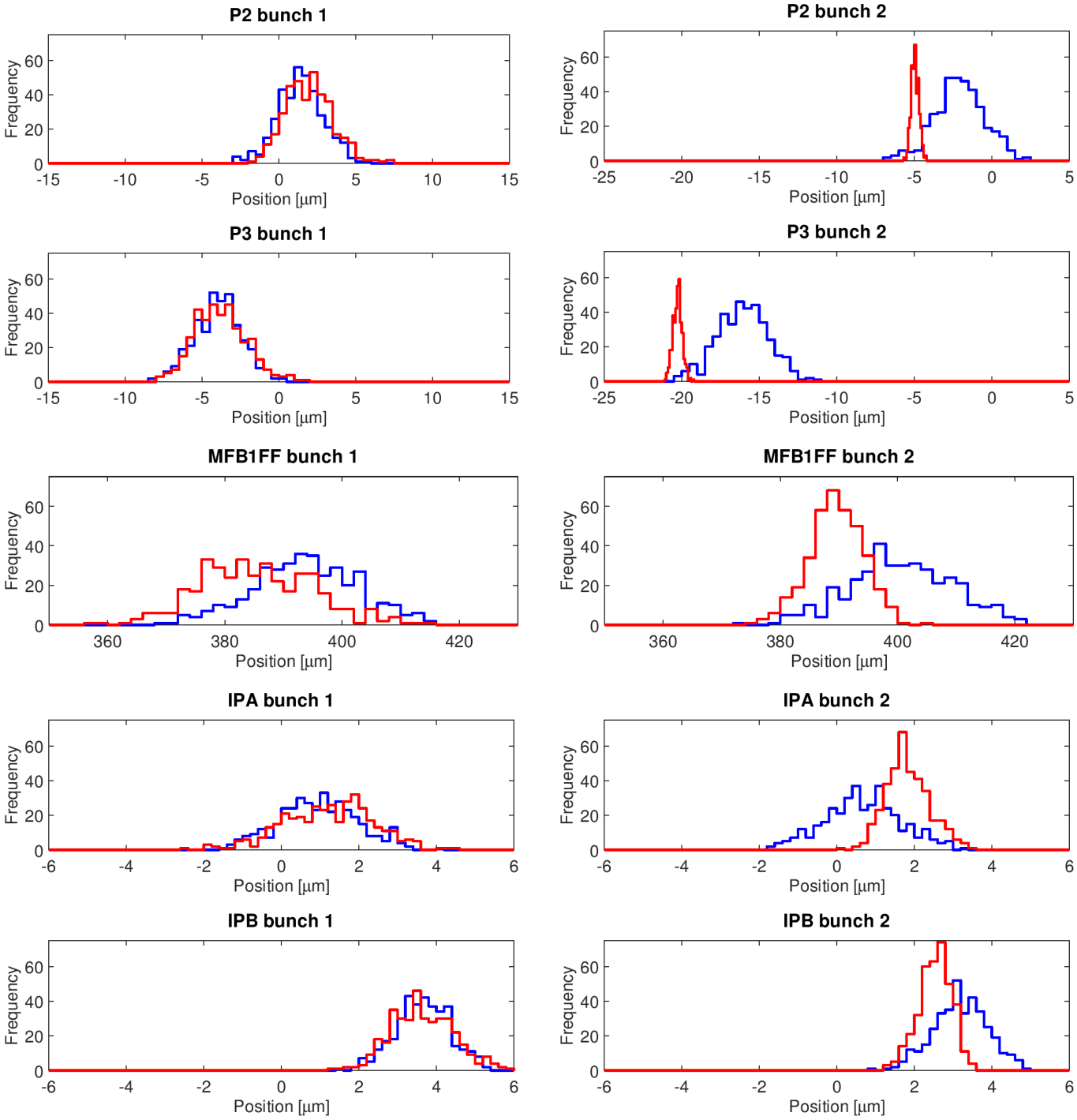

FIG. 4. Distribution of beam positions measured at each BPM with feedback off (blue) and feedback on (red). Each row represents a different BPM and each column a different bunch. A reduced bin width is used for the feedback on data where necessary to limit the maximum frequency of a single bin for aesthetic purposes.

feedback on data sets indicates that the measured reduction in jitter at P2 and P3 is only expected to translate into a factor two reduction of the jitter at each of the witness BPMs, close to what is achieved.

Another metric relevant to the feedback performance is the bunch-to-bunch correlation. Table IV shows the calculated correlation between the measured positions of the two bunches at each BPM. For the three witness BPMs, the corresponding values obtained from the P2 and P3 data tracked downstream using the model are also presented. The measurements suggest that a significant amount of correlation remains at the witness BPMs,

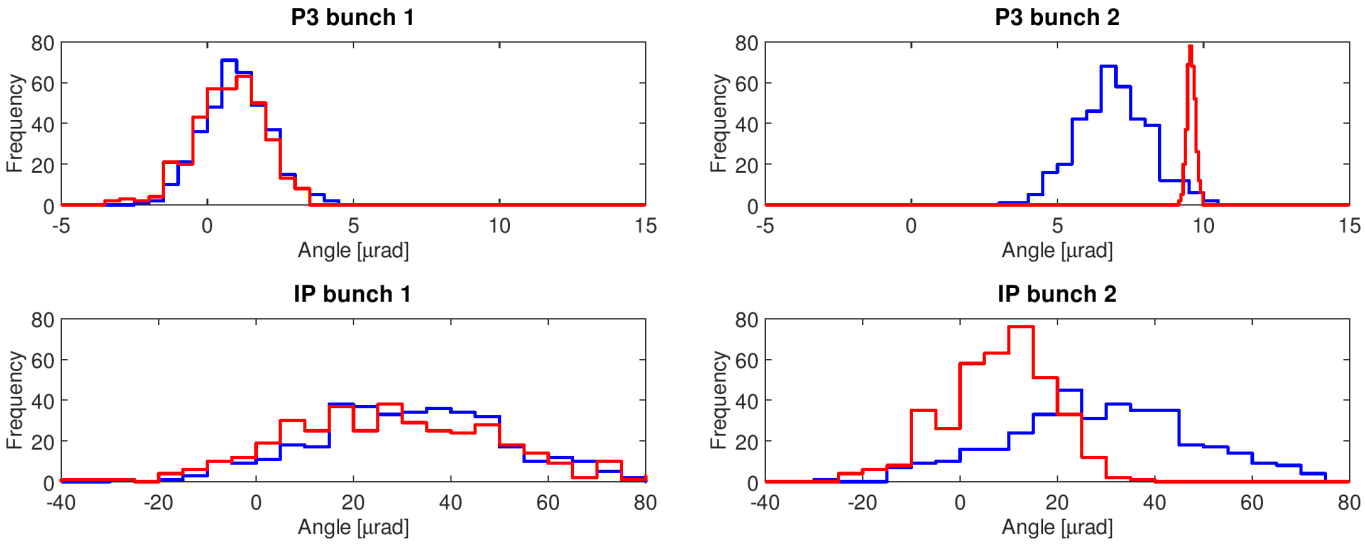

FIG. 5. Distribution of beam angles inferred at P3 (from the positions at P2 and P3) and in the IP region (from the positions at IPA and IPB) with feedback off (blue) and feedback on (red). A reduced bin width is used for the feedback on data where necessary to limit the maximum frequency of a single bin for aesthetic purposes.

despite the large reduction in correlation achieved at the feedback BPMs. The calculated correlation between the inferred angles of the two bunches is also presented in Table **??**. Both sets of results suggest that the model is not entirely accurate as tracking predicts a lower bunch-to-bunch correlation for both position and angle than is actually measured.

Notwithstanding this the model can also be used to predict the beam distribution at the focal point of the machine where the vertical position jitter is at a minimum. The trajectory of the second bunch in the region from IPA to IPB is shown in Figure 6. For the feedback off run, the P2 and P3 data predict a position jitter of 16.0 ± 0.6 nm at the focal point of the beam, which is expected to lie about 2/3 of the distance from IPA to IPB. With feedback operational, the equivalent value at the point of minimum jitter is 2.3 ± 0.1 nm.

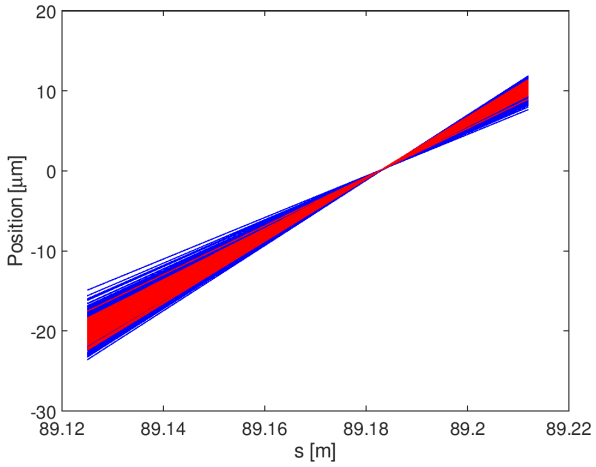

FIG. 6. Trajectory of the second bunch in the IPA to IPB region calculated from the measurements at P2 and P3 for feedback off (blue) and feedback on (red).

IV. CONCLUSIONS

An intra-train position and angle feedback system has been developed for the KEK ATF to achieve the beam stability goal of the ATF2 collaboration. The beam position is measured in real-time using two stripline BPMs and analogue signal-processing electronics. The processed signals are digitized by an FPGA-based digital board which calculates and outputs a pair of correction signals to be applied to the next bunch. The correction signals are sent to two stripline kickers via high-current drive amplifiers. A third stripline BPM located 25 m downstream of the feedback BPMs is also instrumented and used, along with a pair of cavity BPMs located in the region of the notional IP, to determine the effect of the feedback correction downstream of the feedback BPMs themselves.

Operating on a train of two bunches separated by 187.6 ns, the feedback system stabilized the position at the feedback BPMs to the 250-300 nm level. Using the measured positions at the feedback BPMs and the model of the beamline, the angle of the beam at the feedback BPMs can be inferred and the feedback system is seen to stabilize it to within 300 nrad. The model further predicts that the level of correction achieved at the feedback BPMs (∼6 for position and ∼9 for angle) should translate to a factor 2 reduction in position and angle at the witness BPM, close to what is observed, and a minimum jitter at the focal point of the machine of approximately

TABLE II. Vertical beam position jitter for both bunches for feedback off and feedback on. The top five rows are measured values and the bottom three rows are the result of tracking the P2 and P3 position data downstream.

Name	Bunch 1 [μm]		Bunch 2 [μm]		Correction
	off	on	off	on	factor
P2	1.49 ± 0.05	1.55 ± 0.06	1.63 ± 0.06	0.25 ± 0.01	6.5
P3	1.54 ± 0.06	1.69 ± 0.06	1.65 ± 0.06	0.30 ± 0.01	5.5
MFB1FF	8.93 ± 0.33	9.75 ± 0.36	8.78 ± 0.32	4.65 ± 0.17	1.9
IPA	1.02 ± 0.04	1.16 ± 0.04	0.98 ± 0.04	0.56 ± 0.02	1.8
IPB	0.70 ± 0.03	0.80 ± 0.03	0.69 ± 0.03	0.42 ± 0.02	1.6
MFB1FF	9.90 ± 0.36	10.12 ± 0.37	10.68 ± 0.39	5.37 ± 0.20	2.0
IPA	1.31 ± 0.05	1.33 ± 0.05	1.41 ± 0.05	0.70 ± 0.03	2.0
IPB	0.64 ± 0.02	0.65 ± 0.02	0.69 ± 0.03	0.35 ± 0.01	2.0

TABLE III. Vertical beam angle jitter for both bunches inferred from the P2 and P3 position data for feedback off and feedback on, tracked to MFB1FF and the IP region. The final row contains the angle inferred in the IP region from the positions measured at IPA and IPB.

Name	Bunch 1 [μrad]		Bunch 2 [μrad]		Correction
	off	on	off	on	factor
P2	1.12 ± 0.04	1.20 ± 0.04	1.22 ± 0.04	0.14 ± 0.01	8.7
P3	1.11 ± 0.04	1.19 ± 0.04	1.21 ± 0.04	0.14 ± 0.01	8.6
MFB1FF	2.15 ± 0.08	2.19 ± 0.08	2.32 ± 0.09	1.15 ± 0.04	2.0
IP	22.3 ± 0.8	22.80 ± 0.8	24.1 ± 0.9	12.0 ± 0.4	2.0
IP	19.6 ± 0.7	22.4 ± 0.8	19.0 ± 0.7	11.0 ± 0.4	1.7

TABLE IV. Bunch-to-bunch position correlation coefficient for feedback off and feedback on. The top five rows are measured values and the bottom three rows are the result of tracking the P2 and P3 position data downstream.

Name	Feedback off	Feedback on
P2	0.99 ± 0.01	0.21 ± 0.05
P3	0.98 ± 0.01	0.06 ± 0.05
MFB1FF	0.98 ± 0.01	0.39 ± 0.05
IPA	0.98 ± 0.01	0.41 ± 0.05
IPB	0.98 ± 0.01	0.48 ± 0.05
MFB1FF	0.87 ± 0.03	-0.27 ± 0.05
IPA	0.88 ± 0.03	-0.27 ± 0.05
IPB	0.87 ± 0.03	-0.28 ± 0.05

TABLE V. Bunch-to-bunch angle correlation coefficient for feedback off and feedback on calculated from the P2 and P3 position data and the model. The final row contains the correlation for the angle inferred in the IP region from the positions measured at IPA and IPB.

Name	Feedback off	Feedback on
P2	0.99 ± 0.01	0.29 ± 0.05
P3	0.99 ± 0.01	0.28 ± 0.05
MFB1FF	0.88 ± 0.03	-0.27 ± 0.05
IP	0.88 ± 0.03	-0.27 ± 0.05
IP	0.99 ± 0.01	0.45 ± 0.05

2 nm, meeting the beam stability goal of the ATF2 collaboration.

V. ACKNOWLEDGMENTS

We thank the KEK ATF staff for their outstanding logistical support and for providing the beam time and the necessary stable operating conditions for this research. In addition, we thank our colleagues from the ATF2 collaboration for their help and support. In particular, we thank the IFIC group from the University of Valencia for providing the BPM mover system. We acknowledge financial support for this research from the United Kingdom Science and Technology Facilities Council via the John Adams Institute, University of Oxford, and CERN, CLIC-UK Collaboration, Contract No. KE1869/DG/CLIC. The research leading to these results has received funding from the European Commission under the Horizon 2020/Marie Skłodowska-Curie Research and Innovation Staff Exchange (RISE) project E-JADE, Grant Agreement No. 645479.

[1] R. J. Apsimon, D. R. Bett, N. B. Kraljevic, P. N. Burrows, G. B. Christian, C. I. Clarke, B. D. Constance, H. D. Khah, M. R. Davis, C. Perry, J. R. López, and C. J.

Swinson, Phys. Rev. ST Accel. Beams **18** (2015), 032803.
[2] R. J. Apsimon, D. R. Bett, N. B. Kraljevic, R. M. Bodenstein, T. Bromwich, P. N. Burrows, G. B. Christian, B. D. Constance, M. R. Davis, C. Perry, and R. Ramjiawan, Phys. Rev. Accel. Beams **21** (2018), 122802.
[3] Y. Inoue, H. Hayano, Y. Honda, T. Takatomi, T. Tauchi, J. Urakawa, S. Komamiya, T. Nakamura, T. Sanuki, E. S. Kim, S. H. Shin, and V. Vogel, Phys. Rev. ST Accel. Beams **11** (2008), 062801.